Origin, branching pattern, foraminal and intraspinal distribution of the human lumbar sinuvertebral nerves

Breemer, M.C.; Malessy, M.J.A.; Notenboom, R.G.E.

ELSEVIER

The SPINE JOURNAL

The Spine Journal 000 (2021) 1–11

Basic Science

Origin, branching pattern, foraminal and intraspinal distribution of the human lumbar sinuvertebral nerves

Marcus C. Breemer, MD[a], Martijn J.A. Malessy, MD, PhD[a], Robbert G.E. Notenboom, PhD[b,*]

[a] *Department of Neurosurgery, Leiden University Medical Center, Leiden, The Netherlands*
[b] *Department of Anatomy & Embryology, Leiden University Medical Center, Leiden, The Netherlands*
Received 7 June 2021; revised 24 October 2021; accepted 25 October 2021

Abstract

BACKGROUND CONTEXT: The lumbar sinuvertebral nerve (SVN) innervates the outer posterior intervertebral disc (IVD); it is thought to mediate discogenic low-back pain (LBP). Controversy, however, exists on its origins at higher (L1–L2) versus lower (L3–L5) lumbar levels. Additionally, lack of knowledge regarding its foraminal and intraspinal branching patterns and extensions may lead to iatrogenic damage.

PURPOSE: To systematically describe the origins of the L2 and L5 SVNs, their morphological variation in the intervertebral foramen (IVF) and intraspinal distribution.

STUDY DESIGN: Dissection-based study of 20 SVNs with histological confirmation in five embalmed human cadavers.

METHODS: The origin, branching pattern and distribution of the L2 and L5 SVNs was investigated bilaterally in five human cadavers using dorsal and anterolateral dissection approaches. Parameters studied included somatic and/or autonomic SVN root contributions, foraminal SVN morphology and course, diameter, branching point, intraspinal distribution and IVD innervation pattern. Nerve tissue was confirmed by immunostaining for neurofilament and S100 proteins.

RESULTS: The SVN and its origins was identified in all except one IVF at L2 and in all foramina at L5. At L2, the SVN arose in nearly 90% of sides from both somatic and autonomic roots and at L5 in 40% of sides. The remaining SVNs were formed by purely autonomic roots. The SVN arose from significantly more roots at L2 than L5 (3.1 ± 0.3 vs. 1.9 ± 0.3, respectively; p=.022). Four different SVN morphologies could be discerned in the L2 IVF: single filament (22%), multiple (parallel or diverging) filament (33%), immediate splitting (22%) and plexiform (22%) types, whereas the L5 SVN consisted of single (90%) and multiple (10%) filament types. SVN filaments were significantly thicker at L2 than L5 (0.48 ± 0.06 mm vs. 0.33 ± 0.02 mm, respectively; p=.043). Ascending SVN filaments coursed roughly parallel to the exiting spinal nerve root trajectory at L2 and L5. Branching of the SVN into ascending and descending branches occurred mostly intraspinal both at L2 and L5. Spinal canal distribution was also similar for L2 and L5 SVNs. Lumbar posterior IVDs were innervated by the descending branch of the parent SVN and ascending branch of the subjacent SVN.

CONCLUSIONS: The SVN at L2 originates from both somatic and autonomic roots in 90% of cases and at L5 in 40% of cases. The remaining SVNs are purely autonomic. In the IVF, the L2 SVN is morphologically heterogeneous, but generally consists of numerous filaments, whereas at L5 90% contains a single SVN filament. The L2 SVN is formed by more roots and is thicker than the L5 SVN. Intraspinal SVN distribution is confined to its level of origin; lumbar posterior IVDs are innervated by corresponding and subjacent SVNs (ie, two spinal levels).

CLINICAL SIGNIFICANCE: Our findings indicate that L5 discogenic LBP may be mediated both segmentally and nonsegmentally in 40% of cases and nonsegmentally in 60% of cases. Failure of lower lumbar discogenic pain treatment may be the result of only interrupting the nonsegmental pathway, but not the segmental one as well. Relating SVN anatomy to microsurgical spinal approaches may prevent iatrogenic damage to the SVN and the formation of postsurgical back

*Corresponding author. Department of Anatomy & Embryology, Leiden University Medical Center, Zone S1-P, P.O. Box 9600, 2300 RC Leiden, The Netherlands. Tel.: +31 71 526 9352; fax: +31 71 526 8289.
E-mail address: r.g.e.notenboom@lumc.nl (R.G.E. Notenboom).

https://doi.org/10.1016/j.spinee.2021.10.021

Keywords: Afferent pathways; Anatomy; Discogenic low-back pain; Innervation; Intervertebral disc; Intervertebral foramen; Recurrent meningeal nerve; Spinal surgery

Introduction

The sinuvertebral or recurrent meningeal nerve of Luschka (*ramus meningeus nervi spinalis*) [1] is located bilaterally on every vertebral level, innervating the posterior intervertebral disc (IVD) and posterior longitudinal ligament (PLL), vertebral body and pedicles, and associated soft tissues in the intervertebral foramen (IVF) and anterior spinal canal. In humans, the sinuvertebral nerve (SVN) has been described at cervical [2−7], thoracic [2,3,6,8,9], lumbar [3,6,8−14] and sacral [2,6,9,11] levels, but in greatest detail in the lumbar region (for a recent review, see [15]).

In the classic pattern, the SVN receives a somatic contribution from the spinal nerve or its ventral ramus and an autonomic contribution from the gray ramus communicans, which unite to form a single SVN proper that continues medially in the IVF [8,12]. The SVN is located ventral to the dorsal root ganglion (DRG) in the ventral portion of the IVF, and generally travels alongside the spinal branch of the lumbar artery. Lateral to the PLL, the SVN splits into an ascending and a lesser descending branch, which may or may not have multisegmental ramifications and interconnect with sub- and superjacent SVNs [3,6,9].

Clinically, the SVN is important because it is the most likely mediator of discogenic low-back pain (LBP). In Western countries, chronic LBP is the leading cause of disability, with a large individual and societal burden; its costs are estimated to be 1%-2% of the gross national product [16,17]. The intervertebral disc is the primary pain generator in approximately 25% of chronic LBP cases [18]. The exact role of the SVN in the generation of (discogenic) LBP is not yet fully determined. Surgery in the lumbosacral spinal region frequently leads to LBP [19], which may be caused by unintentional SVN damage during exploration.

Murine studies indicate that lower lumbar discogenic pain is mediated by two separate pain pathways: segmentally via the somatic SVN root to its corresponding level DRG neurons, and nonsegmentally via the autonomic SVN root, with nociceptive fibers ascending through gray rami communicantes and the sympathetic trunk to L1−L2 DRG neurons [20−24]. It is not known whether L5 LBP in humans is similarly transmitted nonsegmentally to L1−L2 DRGs. Remarkably, the murine model is used to justify several therapies, which presumably target the nonsegmental pathway, frequently with disappointing results [25,26].

Thus far, cadaver studies on the origin of the human lumbar SVNs have produced conflicting results, with some studies finding exclusively autonomic SVN origins at all lumbar levels [6] and others indicating a classic dual root SVN origin at higher lumbar (L1−L2) levels, but a purely autonomic one at lower lumbar (L3−L5) levels [13]. More recently, Zhao et al. [14] reported both origins, but their study does not indicate if a dual root lumbar origin coexists, nor if the somatic and/or autonomic root contributions differ per lumbar level.

Precise knowledge of lumbar SVN origins is, however, crucial to unraveling discogenic LBP pathways and in treating it. We therefore studied the lumbar anatomy of the SVN and specifically focused on its somatic and/or autonomic origins at higher (L2) vs lower (L5) lumbar levels. Additionally, we provide a detailed description of its foraminal and intraspinal branching pattern and distribution at these lumbar levels.

Materials and methods

Anatomic dissection

Microanatomic dissections of the lumbar SVNs were performed in 5 embalmed human Caucasian cadavers (2 male, 3 female; mean age, 70.0 ± 8.5 years [range, 37−85 years]) obtained from body donation. All donors signed Donor Consent forms in accordance with institutional guidelines and the Dutch Burial and Cremation Act. None of the cadavers had externally visible lumbar abnormalities. Embalmment was within 36 hours after death by femoral artery perfusion with a 2%−4% formaldehyde fixation solution.

Dissections were performed using a Zeiss Universal S2 operating microscope (Carl Zeiss AG, Oberkochen, Germany) at 4−40x magnification. The L2 and L5 SVNs were dissected bilaterally. Photographs were taken with a Sony Cybershot DSC-H50 (Tokyo, Japan) or a Canon EOS 10D (Tokyo, Japan) camera.

Dorsal and anterolateral approaches were used. In the dorsal approach, after removal of the skin and paravertebral muscles, laminectomies, facetectomies and pediculectomies were performed bilaterally from L1−S1. The anterior L2 and L5 spinal canal and IVF was exposed by resection of the spinal cord and dura mater, and retraction of the dural root sleeve and DRG. The SVN was meticulously dissected and freed from the surrounding adipose tissue and vasculature to reveal its ramifications and to note its anatomical relationships. The ascending and descending SVN branches were isolated from the extensive anterior internal vertebral venous plexus and traced as far as possible cranially, caudally and medially. Dural branches were not traced further. Careful dissection at high magnification was performed laterally in the IVF to trace the somatic and autonomic SVN origins.

An anterolateral approach to the lateral IVF was used to further trace the SVN roots. After removal of the viscera and identification of the sympathetic trunk and rami communicantes, the psoas major muscle was resected from its vertebral origins to trace the communicating rami to their junction with the ventral spinal ramus, just lateral to the IVF. Transforaminal ligaments [27] were identified, and where possible, conserved.

SVN roots were counted and designated somatic if they macroscopically originated from the ventral ramus, spinal nerve or DRG, autonomic if they arose from the gray ramus communicans, and typed as junctional if they exited at the ramus communicans-spinal nerve junction. No macroscopic distinction between somatic and autonomic could be made in the latter. The distances between the somatic SVN root exit and the distal DRG pole were measured, and between the autonomic SVN root exit and the gray ramus communicans-spinal nerve junction (Fig. 1). The distal DRG pole was determined using its lateral convexity margin and gray coloration relative to the spinal nerve. Other measurements included thickest (foraminal) SVN filament diameter, angle between the longitudinal axis of the SVN and the transverse anatomical plane, and the SVN branching point; distance of SVN splitting into an ascending and descending branch, relative to the superjacent medial pedicle border (ie, central canal, subarticular or foraminal zone branching) (Fig. 1). Foraminal SVN distribution types and IVD (SVN) innervation patterns were noted. When multiple SVN filaments were present, the diameter of the thickest filament was measured. Filament thickness and distances were measured with a half-millimeter ruler; values for filament thickness were determined at 10x magnification and rounded to the nearest 0.1 mm. Angles were measured with a protractor. Axial lumbar zonal terminology adhered to the nomenclature by Fardon et al. [28]; intraspinal denotes both the central canal and subarticular zones.

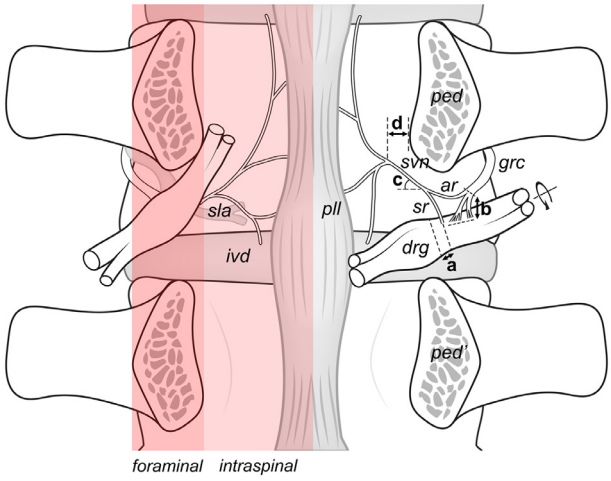

Fig. 1. Schematic illustration of the parameters measured. Dorsal view of anterior vertebral canal after removal of posterior arches, zygapophyseal joints and spinal cord with dura, and clockwise rotation of the spinal roots-dorsal root ganglion (DRG)-spinal nerve complex. Measurements included: (a) distance between the somatic root exit of the sinuvertebral nerve (SVN) and the distal DRG pole, (b) distance between the autonomic SVN root exit and the gray ramus communicans-spinal nerve junction, (c) related acute angle between the longitudinal axis of SVN and the transverse anatomical plane, and (d) branching point as defined by the distance of SVN splitting into an ascending and descending branch, relative to the superjacent medial pedicle border. Foraminal indicates foraminal zone (shaded dark red) and intraspinal denotes subarticular and central canal zones (shaded light red). ar, autonomic SVN root; drg, dorsal root ganglion; grc, gray ramus communicans; ivd, intervertebral disc; ped, pedicle; ped', subjacent pedicle; pll, posterior longitudinal ligament; svn, sinuvertebral nerve; sr, somatic SVN root; sla, spinal branch of the lumbar artery. (Color version of figure is available online.)

Tissue processing and histology

Samples from all dissected SVNs were embedded in paraffin, cut into 7-μm thick serial sections and mounted on poly-L-lysine-coated glass slides (VWR International, Radnor, PA). Tissue sections were dewaxed and either stained with hematoxylin and eosin (HE) or immunostained with a monoclonal mouse anti-neurofilament protein antibody (1:400; clone 2F11; M0762; Dako Denmark A/S, Glostrup, Denmark) (staining of axons) or a polyclonal rabbit anti-S100 serum (1:20,000; Z0311; Dako Denmark A/S) (staining of Schwann cells) to confirm their neural tissue content.

Antibody binding was detected using the avidin-biotin complex (ABC) method [29] with a Vectastain Elite ABC Kit (PK-6100; Vector Laboratories, Inc., Burlingame, CA) and 3,3'-diaminobenzidine tetrahydrochloride (0.05% in 50 mM Tris-HCl, pH 7.0, containing 0.01% H_2O_2; Sigma-Aldrich, St. Louis, MO) as chromogen. Endogenous peroxidase activity was quenched with 3% H_2O_2 in methanol for 20 minutes. Primary antisera were diluted in phosphate-buffered saline (PBS; pH 7.4) containing 1% bovine serum albumin (BSA) and applied overnight at room temperature. Second layer antisera included biotinylated rabbit anti-mouse (1:200; E0354; Dako Denmark A/S) and biotinylated swine anti-rabbit (1:400; E0353; Dako Denmark A/S) IgG serum and were applied in PBS/1% BSA for 1 hour each. After all incubations, the sections were rinsed three times in PBS for 5 minutes. Sections were lightly counterstained with hematoxylin, dehydrated, mounted, and coverslipped.

Except for one L2 sample (left side), which appeared to be a vascular structure surrounded by connective tissue strands and was therefore excluded from our analyses, all other resection tissue (n=19) was neural tissue, containing both myelinated and nonmyelinated nerve fibers (Fig. 2).

Statistical analysis

Statistical analyses were performed with SPSS version 25 (IBM, Armonk, NY) using an independent samples *t* test (parametric data) or a Mann-Whitney *U* test (nonparametric data). A Kruskal-Wallis test (nonparametric data) with post hoc Bonferroni correction was used for multiple-group comparisons. Parametric assumptions were tested using the Shapiro-Wilk test of normality, Z-scores and Levene's test

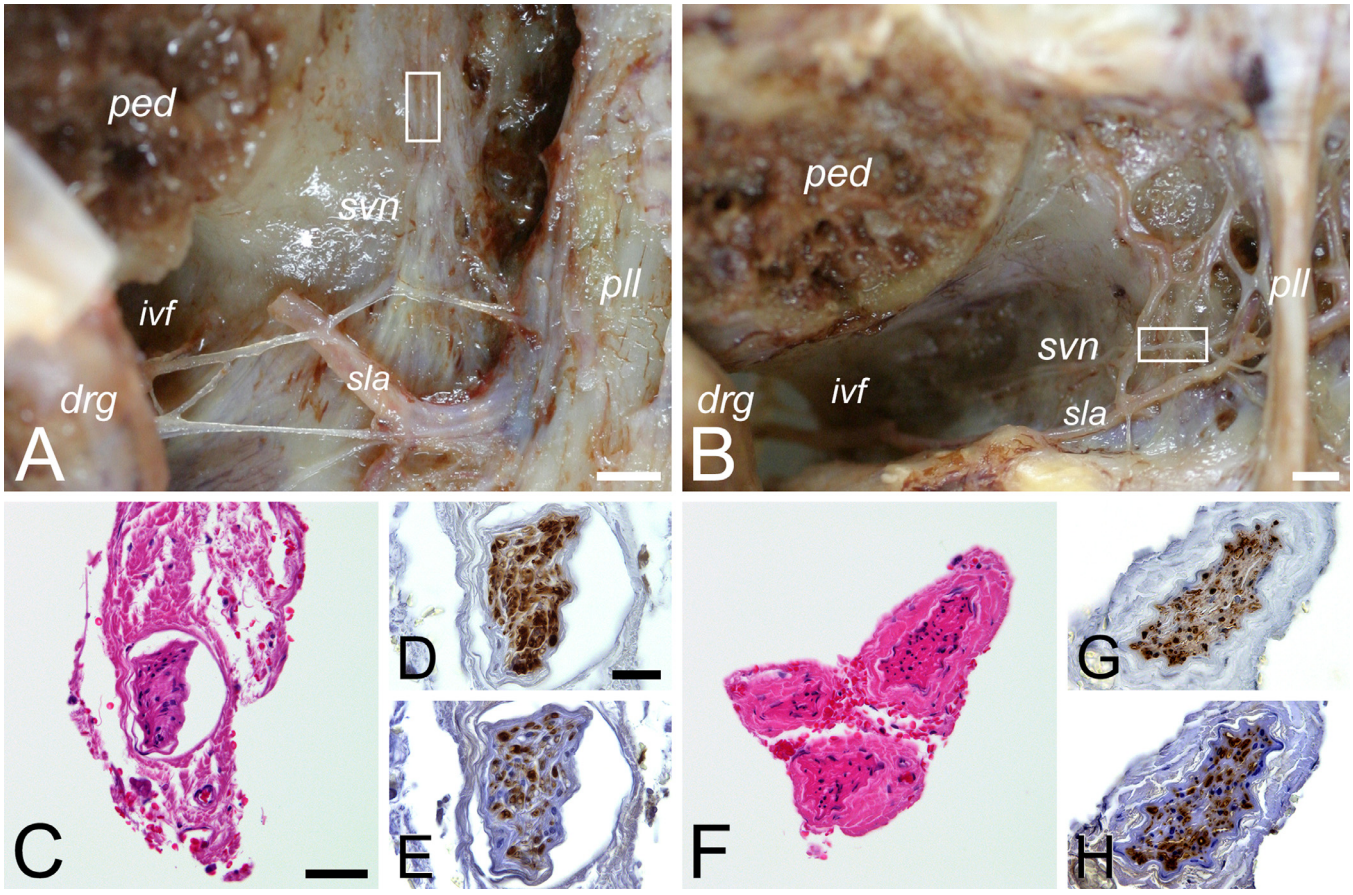

Fig. 2. Histological characterization of L2 and L5 sinuvertebral nerves. Tissue samples from microdissected sinuvertebral nerves (SVNs) were verified for nerve tissue using hematoxylin and eosin (HE) staining and immunostaining for neurofilament (neuronal marker) and S100 (Schwann cell marker) proteins. (A,B) Dorsal view of L2 (A) and L5 (B) SVNs in the anterior intervertebral foramen (IVF) and vertebral canal after removal of the posterior arches, zygapophyseal joints and spinal cord with dura, pedicle reduction, and retraction of the dorsal root ganglion (DRG). (A) Plexiform type SVN; ascending branch (left side). (B) Single filament type SVN; SVN proper (left side). (C–H) Tissue sections taken from the level indicated by the box in A (C–E) and B (F–H) and stained with HE (C,F), and for S100 protein (D,G) and neurofilament protein (E,H). drg, dorsal root ganglion (retracted laterally); ivf, intervertebral foramen; ped, pedicle; pll, posterior longitudinal ligament; svn, sinuvertebral nerve; sla, spinal branch of the lumbar artery. Scale bar: 2 mm (A and B); 50 μm (C and F); 25 μm (D,E,G and H).

of equality of variances. Because left- and right-sided data per level (number of roots, filament diameter and branching point) did not differ significantly, pooled data were analyzed for inter- or intra-level differences. Metric data are presented as mean ± SEM values, categorical data by frequency and percentage. p Values <.05 were considered significant. Scatter plots were computed using GraphPad Prism version 8.4.2 (GraphPad Software, Inc., San Diego, CA).

Results

L2 SVN origins

At L2, a SVN and its origins was identified in all IVFs. No L2 SVN was formed purely by somatic or autonomic roots. Six out of 9 SVNs (66.7%; 3 right sides, 3 left sides) arose from both somatic and autonomic roots (Fig. 3A, E). Two SVNs (22.2%; 1 right side, 1 left side) arose from somatic, autonomic and junctional roots (Fig. 3C), and 1 SVN (11.1%; 1 right side) was formed by somatic and junctional roots (summarized in Table 1). The SVN was composed of up to 4 roots, on average by 3.1 ± 0.3 roots (range, 2–4 roots; n=9 SVNs) (Table 2). The somatic contribution usually arose from the spinal nerve at a distance ranging from 1.0 to 10.0 mm (mean, 3.67 ± 0.89 mm; n=9) to the distal DRG. Once, a somatic root exited 3.0 mm proximal to the distal DRG (ie, from the DRG itself) (right side). The autonomic root arose from the gray ramus communicans at a distance ranging from 2.0–8.0 mm (mean, 4.75 ± 0.73 mm; n=8) from the ramus communicans-spinal nerve junction. No SVN origins from the paravertebral sympathetic ganglia or sympathetic trunk were found.

L2 foraminal SVN morphology

Four SVN types were found in the IVF after its roots conjoined (summarized in Fig. 4): single filament on 2 of 9 sides (22.2%; 1 right side, 1 left side) (Fig. 4A; cf. Fig. 3A), multiple filament (up to 3; parallel or diverging) on 3 of 9

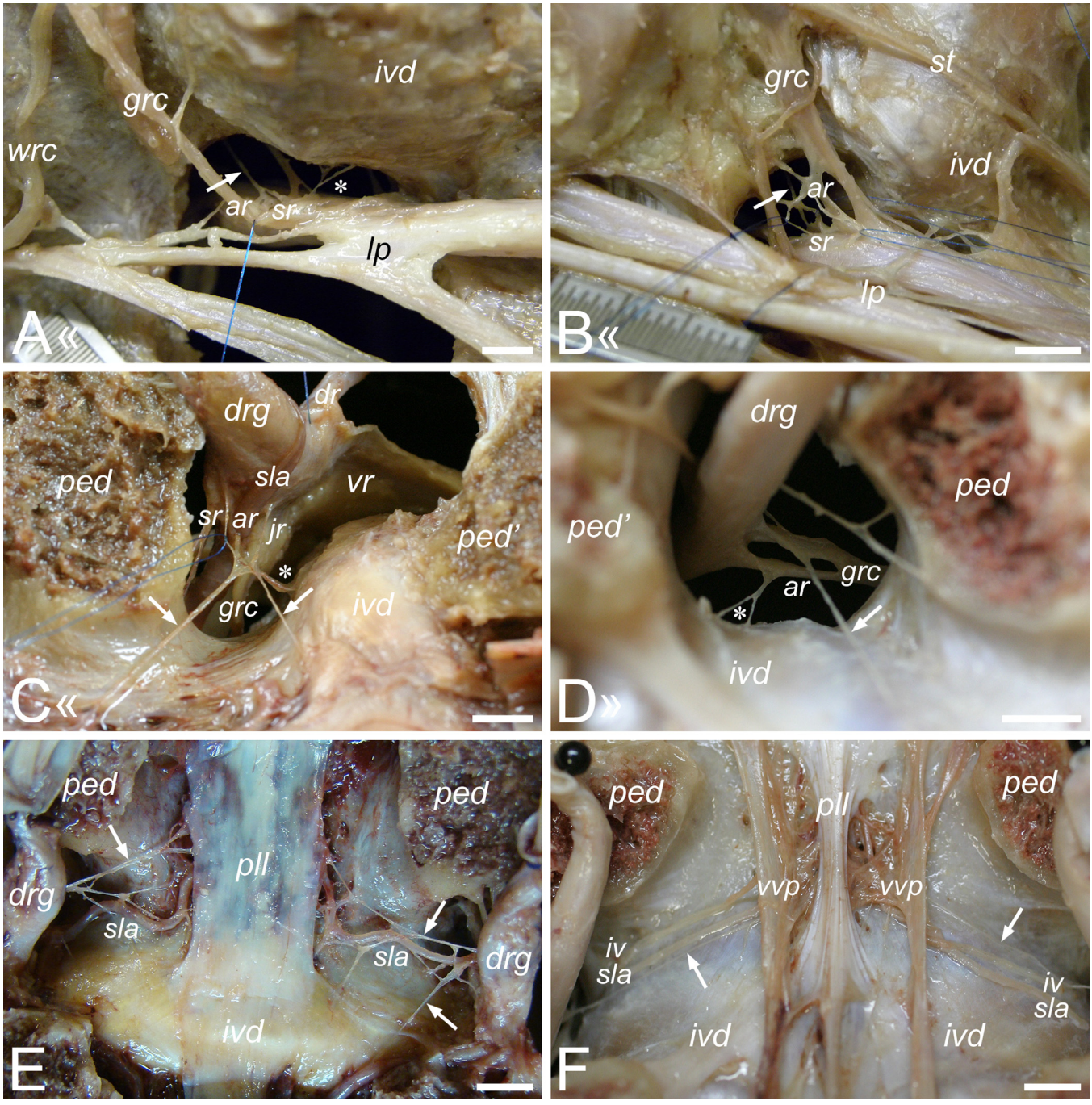

Fig. 3. Origin and course of the L2 and L5 sinuvertebral nerve. (A,B) Ventrolateral, (C,D) dorsolateral and (E,F) dorsal views of L2 (A,C,E) and L5 (B,D,F). (A) Dual (somatic and autonomic) L2 sinuvertebral nerve (SVN) origin. Ventrolateral view of the L2 intervertebral foramen (IVF) after resection of the psoas major muscle; the gray ramus communicans is retracted. Single filament type SVN (arrow) formed by two somatic roots and one autonomic root. (B) Dual (somatic and autonomic) L5 SVN origin, found in 40% of sides. Ventrolateral view of the L5 IVF after resection of the psoas major muscle; outer somatic SVN roots pulled apart and gray ramus communicans partly retracted. Single filament type SVN (arrow) formed by three somatic roots and one autonomic root. (C) Classic dual (somatic and autonomic) L2 SVN origin, found in 88.9% of sides. Dorsolateral view of the right L2 IVF from within the spinal canal with the dorsal root ganglion (DRG) and somatic SVN root retracted with monofilament suture, and the spinal branch of the lumbar artery reflected onto the DRG. Immediate splitting type SVN (arrows). After root convergence into SVN proper, immediate splitting into an ascending and descending branch. Note additional junctional root emerging from the ramus communicans-spinal nerve junction. (D) Pure autonomic L5 SVN origin, found in 60% of sides. Dorsolateral view of the left L5 IVF from within the spinal canal with the DRG retracted. The autonomic root continues as a single filament type SVN (arrow). (E) Foraminal and intraspinal distribution of the L2 SVN. Dorsal view of the L2–L3 anterior epidural space. Immediate splitting (left side) and plexiform (right side) type SVNs (arrows). The SVN courses in the superior or middle anterior portion of the IVF, ramifies around the spinal branch of the lumbar artery and forms a plexus lateral to the posterior longitudinal ligament (PLL), innervating both the PLL and sub-/superjacent intervertebral discs (IVDs). (F) Foraminal and intraspinal distribution of the L5 SVN. Dorsal view of the L5–S1 anterior epidural space. Single filament type SVNs (left and right side; arrows). Bilateral intraspinal branching points, located deep to the anterior internal vertebral venous plexus. Asterisk in A, C and D indicates IVD nerve branches from

Table 1
Sinuvertebral nerve root origins (%) at L2 and L5

Root origin(s)	L2 (n=9)	L5 (n=10)
Somatic only	np	np
Autonomic only	np	60
Somatic and autonomic	66.7	30
Somatic and junctional*	11.1	10
Somatic, autonomic and junctional*	22.2	np

* Roots were typed as junctional if they exited at the gray ramus communicans-spinal nerve junction. np, not present.

Table 2
Sinuvertebral nerve characteristics at L2 and L5

Parameter	L2 Mean ± SEM (Range) n	L5 Mean ± SEM (Range) n	p Value*
Number of roots	3.1 ± 0.3 (2 to 4) 9	1.9 ± 0.3 (1 to 4) 10	**.022**
Somatic roots†	1.4 ± 0.2 (1 to 2) 9	0.7 ± 0.3 (0 to 3) 10	.053
Autonomic roots†	1.3 ± 0.3 (0 to 3) 9	1.1 ± 0.2 (0 to 2) 10	.661
Junctional roots‡	0.3 ± 0.2 (0 to 1) 9	0.1 ± 0.1 (0 to 1) 10	.400
Diameter thickest filament (mm)	0.48 ± 0.06 (0.2 to 0.8) 9	0.33 ± 0.02 (0.2 to 0.4) 10	**.043**
Foraminal filament angle (˚)			
Ascending filament	36.0 ± 4.8 (20 to 45) 5	22.0 ± 3.5 (10 to 35) 10	**.040**
Descending filament	−16.7 ± 1.7 (−20 to −15) 3	np	NA
Branching point (mm)§	0.57 ± 1.63 (−6.0 to 5.0) 7	4.63 ± 1.22 (0.0 to 10.0) 8	.065

NA, not applicable; np, not present.

* p Values <.05 were considered significant; independent samples *t* test (branching point) or Mann-Whitney *U* test (number of roots and root types, diameter, ascending filament angle).

† The number of somatic vs autonomic roots at L2 or L5 did not differ (p=1.000 and p=.227, respectively; Kruskal-Wallis test with post hoc Bonferroni correction).

‡ Roots were typed as junctional if they exited at the gray ramus communicans-spinal nerve junction.

§ Relative to superjacent medial pedicle border.

sides (33.3%; 2 right sides, 1 left side) (Fig. 4B), immediate splitting after union of roots on 2 of 9 sides (22.2%; 1 right side, 1 left side) (Fig. 4C; cf. Fig. 3C, E, left side), and plexiform configurations on 2 of 9 sides (22.2%; 1 right side, 1 left side) (Fig. 4D; cf. Fig. 3E, right side).

Most commonly (6 of 9 sides), the SVN was located in the superior portion of the IVF (66.7%; 4 right sides, 2 left sides) and ran predominantly superior to the spinal branch of the lumbar artery. All SVNs and their branches were located ventral to the DRG; none were found in the dorsal IVF. The mean diameter of the thickest SVN filament was 0.48 ± 0.06 mm (range, 0.2–0.8 mm; n=9) (Table 2; Fig. 5A). Ascending foraminal SVN filaments (5 of 9 sides, 55.6%; 3 right sides, 2 left sides) coursed roughly parallel but recurrent to the exiting spinal nerve root trajectory at a mean angle of 36.0˚±4.8˚ (range, 20˚–45˚; n=5) relative to the transverse anatomical plane (Table 2). Descending L2 SVN filaments (3 of 9 sides, 33.3%; 3 right sides) coursed at a mean angle of −16.7˚±1.7˚ (range, −20˚ to −15˚; n=3) (Table 2). Ascending and descending filaments included single filament, multiple filament (parallel and diverging) and immediate splitting SVN types.

L2 SVN branches to the posterolateral L2/3 IVD were found on 1 of 9 sides (11.1%; right side) (Fig. 3C). Three other sources innervated the posterolateral L2/3 IVD: the gray ramus communicans on 3 of 9 sides (33.3%; 1 right side, 2 left sides), the ventral spinal ramus on 3 of 9 sides (33.3%; 1 right side, 2 left sides) (Fig. 3A) and the spinal nerve on 1 of 9 sides (11.1%; left side). The posterolateral L2 vertebral body and its periosteum received L2 SVN branches on 2 of 9 sides (22.2%; 2 left sides) and from two other sources: the gray ramus communicans on 3 of 9 sides (33.3%; 1 right side, 2 left sides) and the spinal nerve on 1 of 9 sides (11.1%; left side). Of these, one side (11.1%; left side) contained branches from all three sources.

L2 SVN spinal canal distribution

Branching of the L2 SVN into ascending, descending and transverse branches occurred in the foraminal zone on 3 of 7 sides (42.9%; 1 right side, 2 left sides) and intraspinal on 4 of 7 sides (57.1%; 3 right sides, 1 left side) (Fig. 5B). On average, branching occurred 0.57 ± 1.63 mm (range, −6.0 to 5.0 mm; n=7 SVNs) intraspinal to the superjacent medial pedicle border (Table 2; Fig. 5B). These SVN branches formed a plexus lateral to the PLL, ran perivascular to ramifications of the spinal branch of the lumbar artery and either intertwined with or coursed mostly ventral to the anterior internal vertebral venous plexus (Fig. 3E). Ascending, transverse, and descending SVN branches disappeared under the PLL (Fig. 3E), and occasionally entered the basivertebral foramen or into separate small paramedian foramina, together with the basivertebral vein and branches of the spinal branch of the lumbar artery. Small non SVN-derived nerve fibers (cf. [30]) were not found in the IVF or spinal canal.

When present, the ascending SVN branch was generally directed superiorly (8 of 9 sides; 88.9%, 5 right sides, 3 left sides), running to the posterior aspect of the L1/2 IVD on 3

ventral ramus of spinal nerve, SVN, and gray ramus communicans, respectively. ar, autonomic SVN root; dr, dorsal ramus of spinal nerve; drg, dorsal root ganglion (retracted laterally); grc, gray ramus communicans; iv, intervertebral vein; ivd, intervertebral disc; jr, junctional SVN root; lp, lumbar plexus; ped, pedicle; ped', subjacent pedicle; pll, posterior longitudinal ligament; sr, somatic SVN root; sla, spinal branch of the lumbar artery; st, sympathetic trunk; vr, ventral ramus of spinal nerve; vvp, anterior internal vertebral venous plexus; wrc, white ramus communicans. Double sideways chevrons indicate cranial direction. Scale bar=5 mm.

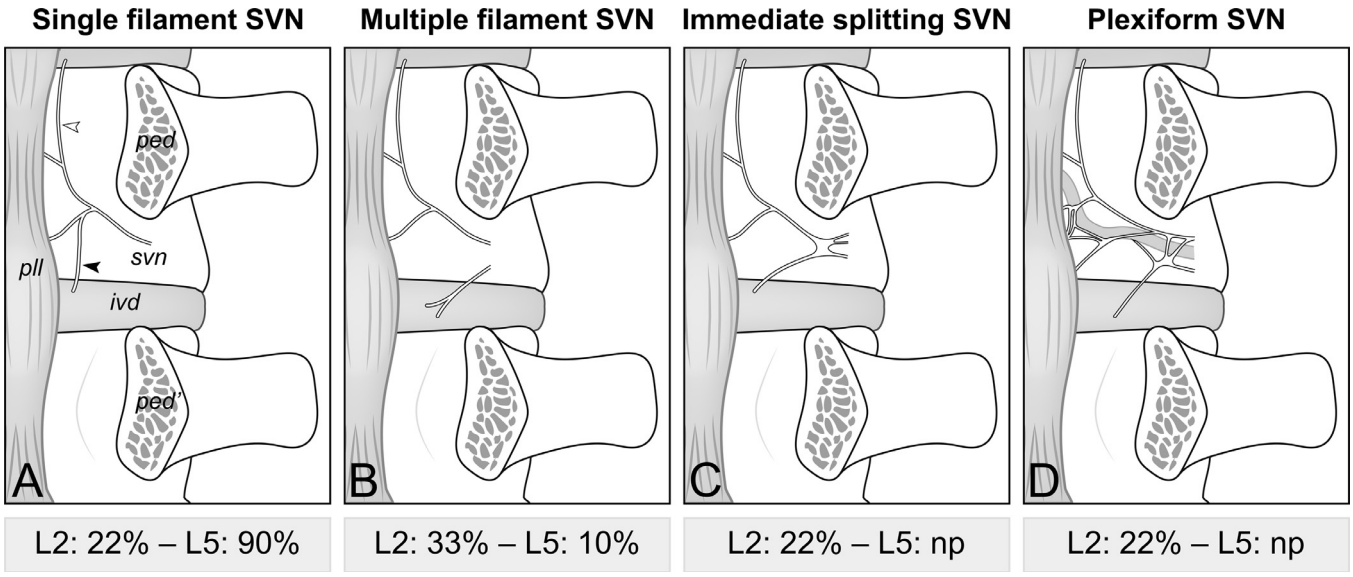

Fig. 4. Foraminal sinuvertebral nerve types and frequencies (%) at L2 and L5. Dorsal view of anterior vertebral canal after removal of posterior arches, zygapophyseal joints and spinal cord with dura, and removal of the spinal roots-dorsal root ganglion-spinal nerve complex. Four distinct foraminal sinuvertebral nerve (SVN) types are recognized: (A) single filament, (B) multiple filament (parallel or diverging), (C) immediate splitting, and (D) plexiform types. At L2, all four SVN types (A–D) are found, whereas at L5 only single (A) or multiple filament (B) type SVNs are present. Note that the descending SVN branch (closed arrowhead) innervates the corresponding (L2/3 or L5/S1) intervertebral disc (IVD), whereas the ascending branch (open arrowhead) innervates the superjacent IVD. ivd, intervertebral disc; ped, pedicle; ped', subjacent pedicle; pll, posterior longitudinal ligament; svn, sinuvertebral nerve.

of 9 sides (33.3%; 1 right side, 2 left sides). It could not be traced beyond this level. The posterior surface of the L2/3 IVD received ramifications from the descending SVN branch on 5 of 9 sides (55.6%; 3 right sides, 2 left sides) (Fig. 3E, C). Sometimes a descending branch coursed between the lateral PLL expansion and L2/3 IVD (Fig. 3E, right side, C), but this could not be traced further caudally. Once, an intersegmental connection between the L2 descending and L3 ascending branch of the SVN was observed. In one specimen, the L2 ascending branch ran at both sides to the L2 basivertebral foramen and the descending L2 branch to the L3 basivertebral foramen. Ascending and descending SVN branches appeared roughly equal in thickness (cf. [12]), although in one specimen the ascending branch seemed markedly thicker.

The cranio- and caudolateral PLL extensions overlaying the IVD received inputs from the parent and superjacent SVN and the parent and subjacent SVN, respectively. The PLL overlaying the vertebral body was innervated by the parent SVN.

L5 SVN origins

At L5, a SVN and its origins was identified in all IVFs. It had purely autonomic origins on 6 of 10 sides (60%; 2 right sides, 4 left sides), usually arising from 1 root (Fig. 3D). On

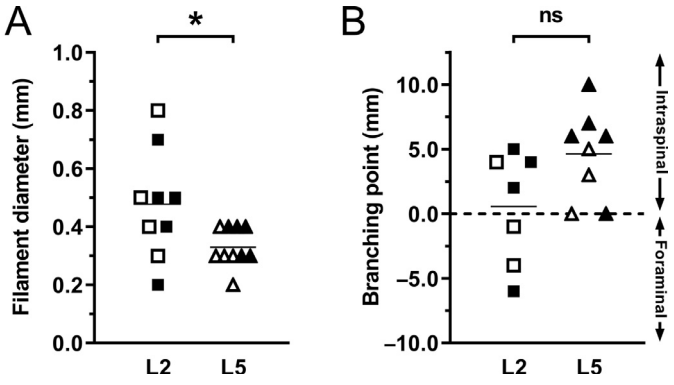

Fig. 5. Scatter plots of (A) sinuvertebral nerve filament thickness (diameter of the thickest filament) and (B) foraminal or intraspinal branching (distance of sinuvertebral nerve splitting into an ascending and descending branch, relative to the superjacent medial pedicle border). Negative values in B indicate foraminal sinuvertebral (SVN) branching; ie, splitting lateral to the medial superjacent pedicle border. Open squares, left-sided L2 SVN; closed squares, right-sided L2 SVN; open triangles, left-sided L5 SVN; closed triangles, right-sided L5 SVN. *p Value <.05; ns, not significant.

3 of 10 sides (30%; 2 right sides, 1 left side), the SVN arose from both somatic and autonomic roots (Fig. 3B); these sides contained more roots than pure autonomic origins: up to 4 (2, 3 and 4, respectively). One side (10%; right side) contained somatic and junctional roots. No SVN had a purely somatic origin at L5. The SVN origins at L5 are summarized in Table 1. On average, the L5 SVN was composed of 1.9 ± 0.3 roots (range, 1–4 roots; n=10 SVNs) (Table 2). The somatic contribution usually arose from the spinal nerve at a distance ranging from 2.0 to 5.0 mm (mean, 2.71 ± 0.42 mm; n=7) to the distal DRG. The autonomic root arose from the gray ramus communicans at a distance ranging from 1.0–6.0 mm (mean, 3.41 ± 0.41 mm; n=11) from the ramus communicans-spinal nerve junction. No SVN origins from the paravertebral sympathetic ganglia or sympathetic trunk were found.

L5 foraminal SVN morphology

A single filament SVN type was found on 9 of 10 sides (90%; 4 right sides, 5 left sides) (Figs. 3B, D, F and 4A), one of which split and reunited while still in the IVF. Except for a multiple filament type SVN (Fig. 4B) on 1 of 10 sides (10%; right side), no other SVN types were found. The SVN ran ventral to the DRG, was usually located superior to the spinal branch of the lumbar artery, and ran in the middle IVF portion on 7 of 10 sides (70%; 4 right sides, 3 left sides). No SVN or its branches was found in the dorsal IVF. The mean diameter of the thickest SVN filament was 0.33 ± 0.02 mm (range, 0.2–0.4 mm; n=10) (Table 2; Fig. 5A). All L5 SVN filaments followed an ascending foraminal course (roughly parallel but recurrent to the exiting spinal nerve root trajectory) at a mean angle of 22.0°± 3.5° (range, 10°–35°; n=10) relative to the transverse anatomical plane (Table 2).

L5 SVN spinal canal distribution

Branching of the L5 SVN into ascending, descending and transverse branches occurred intraspinal on 6 of 10 sides (60%; 4 right sides, 2 left sides) and at the foraminal zone-intraspinal border on 2 of 10 sides (20%; 1 right side, 1 left side). No branching was observed on 2 of 10 sides (20%; 2 left sides). On average, branching occurred 4.63 ± 1.22 mm (range, 0.0–10.0 mm; n=8) intraspinal to the superjacent medial pedicle border (Table 2; Fig. 5B).

No differences in intraspinal SVN distribution were found compared with L2. Transverse branches were traced over the midline multiple times. The ascending branch of the SVN was traced to the posterior L4/5 IVD on 4 of 10 sides (40%; 3 right sides, 1 left side); they could not be traced further than this level with confidence. Ramifications from the descending SVN branch over the L5/S1 IVD were seen on 6 of 10 sides (60%; 4 right sides, 2 left sides) (Fig. 3F). Intersegmental SVN communications were not found. Only once were posterolateral L5/S1 IVD nerve branches seen, originating from the adjacent gray ramus communicans (Fig. 3D). (Peri)osteal L5 nerve branches were found posterolaterally and in the lateral recess, originating from the L5 SVN on 5 of 10 sides (50%; 3 right sides, 2 left sides) or from the DRG on 1 of 10 sides (10%; left side). Osteal branches entered the L5 vertebra via small foramina, sometimes alongside a small arterial branch.

Discussion

In the present study, we examined the anatomy of the SVN at high (L2) and low (L5) lumbar levels, with special focus on its somatic and autonomic origins. This knowledge is important for unraveling the ‘wiring diagram’ of discogenic LBP, and hence, to improve targeting of treatment modalities. Furthermore, it may contribute to preventing iatrogenic damage to the SVN during (transforaminal) surgical approaches to the lumbar spine. Our data show that a dual root origin is common at L2 and that at L5 there is autonomic root predominance but not exclusivity (Table 1). The finding that about half of L5 SVNs are formed by a dual root origin suggests that lower lumbar discogenic pain may not only be transmitted by nonsegmental neural pathways as is widely accepted in clinical practice [31], but also segmentally.

Origin of the SVN

In our study, nearly 90% of SVNs at L2 arose from both somatic and autonomic roots, confirming findings of most authors [3,8,11–13]. At L5, our results confirm an autonomic root predominance, but not exclusivity, as 40% of L5 SVNs contained an additional somatic component. Macroscopically, the SVN at L5 is thus not always purely autonomic as previously reported [6,13].

These discrepancies in previously reported SVN origins might be explained by differences in methodology or dissection techniques to study the SVN; notably lower lumbar SVN roots are difficult to visualize. In human fetuses, Groen et al. [6] using an acetylcholinesterase whole-mount method found that except for the cervical region, all SVNs are exclusively derived from gray rami communicantes. Expression of acetylcholinesterase in somatic SVN roots, however, might well be a later event during fetal development than in autonomic roots. Furthermore, while we have found a similar plexiform arrangement in the ramus communicans’ termination area as Groen et al. [6], and also what appeared macroscopically as “crossing” fiber bundles to the dorsal ramus, the latter did not contribute to the SVN (cf. [32]). Misidentification by others of these “crossing” fibers as originating from the spinal nerve or ventral ramus has, however, been put forward by Groen et al. [6] as a possible explanation for their finding of an exclusive autonomic SVN origin. Groen et al. [6] also contend that the posterolateral retraction of the DRG-dorsal-ventral rami complex, exposing the anterior IVF, might give the impression that the SVN roots originate from the spinal nerve, but that these are actually autonomic in origin. While individual

root identification is difficult, we have clearly demonstrated somatic contributions to the SVN from the ventral ramus, spinal nerve and DRG both at L2 and L5 (Fig. 3).

In agreement with previous studies [13], the SVN arose from significantly more roots at L2 than L5 (Table 2). The number of somatic vs autonomic roots at L2 did not differ (p=1.000, post hoc Bonferroni correction), nor did it at L5 (post hoc p=.227) (Table 2).

Foraminal SVN morphology

Four different foraminal SVN types could be discerned: single filament, multiple filament, immediate splitting and plexiform types (Fig. 4). Configurations with numerous SVN filaments (multiple filament, immediate splitting and plexiform types) are common at L2 (77.8% of sides), whereas at L5, 90% of sides contained a single SVN filament. Lazorthes et al. [10] described two SVN types: single nerve and multiple independent or interconnecting nerves (corresponding to our multiple filament and plexiform types) without reporting regional variation.

Our results indicate that the SVN is significantly thicker at L2 than L5 (Table 2; Fig. 5A). Since only the thickest filament was measured for all SVN types, we performed a subgroup analysis for single filament SVN types, which confirmed this finding. The difference both in the number of SVN roots and the SVN diameter at L2 vs L5, suggests that level-related differences might exist in SVN nerve fiber count and/or composition (small nociceptive C fibers vs larger proprioceptive Aα fibers). It might also indicate that the L5/S1 IVD is innervated more sparsely than higher lumbar IVDs.

The course of the SVN in the IVF matches existing literature: ventral to the DRG and roughly parallel but recurrent to the exiting spinal nerve root trajectory. SVN filaments generally run superior to the spinal branch of the lumbar artery at L2 and L5, occasionally forming a perivascular nerve plexus. This plexus is different from the previously reported nerve plexus around the radicular branch of the lumbar artery, that arises from the gray ramus communicans at the point of SVN origin [6].

Posterolateral IVD branches from the adjacent SVN were uncommon (1 of 9 sides at L2, none at L5). Posterolateral IVD nerve branches derived predominantly from the adjacent ramus communicans and spinal ventral ramus as previously described by Bogduk et al. [12] and Zhao et al. [14]. Zhao et al. [14] classified these branches as SVNs (type I, "SVN deputy branches"), however, the present study did not, in accordance with Bogduk et al. [12]. More numerous posterolateral IVD nerve branches were found at L2/3 than L5/S1; this too could signify a sparser lower lumbar innervation but might also represent dissection artefacts, as this disc region is difficult to dissect with neural structures in situ. The lateral IVD received branches from the adjacent ramus communicans. SVN branches to the anterior longitudinal ligament (cf. [33]) were not found.

SVN distribution in the spinal canal

The present findings that the intraspinal SVN distribution does not differ at L2 and L5 and that the SVN does not extend beyond its level of origin are in accordance with Luschka's original description [8], Lazorthes et al. [10], and Bogduk et al. [12]. Although branching of the SVN into ascending, descending and transverse branches has been described [6,12], its precise branching point has not been further detailed. Branching occurred intraspinal in the subarticular or central canal zone, and generally more medially at L5 than L2 (Table 2; Fig. 5B), irrespective of SVN type.

The posterior L2/3 and L5/S1 IVDs were innervated ipsilaterally by the descending branch of the parent SVN and ascending branch of the subjacent SVN, that is by two spinal levels. This is in accordance with Lazorthes et al. [10] and Bogduk et al. [12], but in contrast to Groen et al. [6], who found that lumbar posterior IVDs were innervated by the parent, sub- and superjacent SVNs, that is by three levels. Such an arrangement could only be valid if a long descending SVN branch extended to the IVD one level lower, but these were not found in the present study. In one specimen, a L2 descending SVN branch ran to the L3 basivertebral foramen, but this did not extend further caudally, although it could theoretically give off thin branches to the L3/4 IVD. Descending SVN branches passing between the lateral PLL extension and IVD were not traced further, but descending SVN branches from superjacent levels were not found at L2 and L5, neither free lying nor appearing from between the superjacent lateral extension of the PLL and its associated IVD.

Clinical implications

Our results indicate that 60% of L5 SVNs are formed purely by autonomic roots. In the absence of a somatic root contribution, discogenic pain transmission can occur via the subjacent SVN, as an IVD is innervated by two spinal levels (this study). Alternatively, it might be mediated nonsegmentally through the previously described autonomic inflow diversion [20–24], whereby nociceptive fibers from lower lumbar IVDs ascend via the autonomic SVN root through gray rami communicantes and the sympathetic trunk to L1–L2 DRG neurons. So far, however, this neural pathway has only been described in rats and awaits further human study.

Remarkably, current therapies for discogenic LBP specifically aim to target this nonsegmental pathway by interrupting pain transmission through nerve blocks, transection, or radiofrequency lesioning of the L2 DRG, spinal nerve or ramus communicans [25,26,31,34–37]. These interventions are not always effective [25,26]. Since we have found that 40% of SVNs at L5 are formed also by somatic roots, which are presumed to contain segmental nociceptive fibers, interruption of the nonsegmental pathway alone is expected to provide only partial pain reduction and may explain some

of the disappointing results in the aforementioned studies. Interindividual "wiring diagram" variations may thus call for different therapeutic approaches to pain reduction in patients with discogenic LBP.

Although the precise role of the SVN in discogenic LBP has not been fully established yet, data from immunohistochemical studies have clearly revealed that healthy and painful lumbar posterior IVDs are innervated by nociceptive fibers from the SVN, indicating a function in pain perception (reviewed in [15,24,38]). Whether these nociceptive fibers indeed mediate painful stimuli both segmentally and nonsegmentally awaits further (functional) studies. Although performing experiments in humans limits research, with the emergence of novel dyes, such as NeuroVue dyes, histological methods for ex vivo axon tracing have also become available for human postmortem tissue (reviewed in [39]).

The spectrum of transforaminal ligaments found in our study matches previous observations [27]. Amonoo-Kuofi et al. [40] have reported that the SVN is constantly transmitted into the IVF through the compartment created by the deep anterior intraforaminal ligament. In the present study, the SVN proper was not transmitted through a compartment created by trans- or intraforaminal ligaments, although the compartment formed by a superior transforaminal ligament did transmit an autonomic SVN root once at L5. The inconstancy of these ligaments indicates they cannot be used reliably as landmarks for the location of the SVN at the foraminal-extraforaminal border.

The anatomy described in this study also has implications for Kambin's triangular safe zone (described in [41]) and Harms' transforaminal corridor [42], used in (minimally invasive and endoscopic) transforaminal spinal approaches (reviewed in [43]). As the SVN generally courses through the superior part of these triangular safe zones, it effectively truncates them into quadrangular safe zones, if a nerve-sparing approach is sought. Unfamiliarity with these neural relations may lead to iatrogenic SVN damage.

Our results are based on a relatively limited sample size (n=5 cadavers), as is not uncommon in this type of labor-intensive anatomical research [3,6,9,12–14]. Nevertheless, our findings are relevant to spinal surgeons who strive to keep the SVN intact during minimally invasive (foraminal) approaches. Future studies will further determine the full extent of foraminal SVN subtypes and distributions.

Conclusions

At L2, the SVN arises in nearly 90% of sides from both somatic and autonomic roots and at L5 in 40% of sides. The remaining SVNs are formed by purely autonomic roots. Lower lumbar discogenic pain is presumably mediated segmentally via the somatic SVN root and nonsegmentally through the autonomic SVN root; targeting only the nonsegmental pathway may provide incomplete pain reduction. In the IVF, the L2 SVN generally consists of numerous filaments, whereas at L5 90% contains a single SVN filament. Relating SVN anatomy to microsurgical spinal approaches may prevent iatrogenic damage to the SVN and the formation of postsurgical back pain.

Conflict of Interest

The authors declare that they have no competing interests.

Acknowledgments

We thank Ingrid Hegeman-Kleinn for technical assistance with the histology.

This research was supported with funding from the Pain-Less foundation and the Schumacher-Kramer Stichting.

References

[1] FIPAT. Terminologia anatomica. Federative international programme for anatomical terminology; 20192nd ed. Available at: https://fipat.library.dal.ca/ta2. Accessed May 31, 2021.
[2] Hovelacque A. Le nerf sinu-vertébral. Ann Anat Pathol Anat Norm Med Chir 1925;2:435–43.
[3] Edgar MA, Nundy S. Innervation of the spinal dura mater. J Neurol Neurosurg Psychiatry 1966;29(6):530–4. https://doi.org/10.1136/jnnp.29.6.530.
[4] Bogduk N, Windsor M, Inglis A. The innervation of the cervical intervertebral discs. Spine (Phila Pa 1976) 1988;13(1):2–8. https://doi.org/10.1097/00007632-198801000-00002.
[5] Chen XQ, Bo S, Zhong SZ. Nerves accompanying the vertebral artery and their clinical relevance. Spine (Phila Pa 1976) 1988;13(12):1360–4. https://doi.org/10.1097/00007632-198812000-00006.
[6] Groen GJ, Baljet B, Drukker J. Nerves and nerve plexuses of the human vertebral column. Am J Anat 1990;188(3):282–96. https://doi.org/10.1002/aja.1001880307.
[7] Rennie C, Haffajee MR, Ebrahim MA. The sinuvertebral nerves at the craniovertebral junction: a microdissection study. Clin Anat 2013;26(3):357–66. https://doi.org/10.1002/ca.22105.
[8] Luschka H. Die Nerven des menschlichen Wirbelkanales. Tübingen: Verlag der H. Laupp'schen Buchhandlung; 1850.
[9] Pedersen HE, Blunck CF, Gardner E. The anatomy of lumbosacral posterior rami and meningeal branches of spinal nerves (sinu-vertebral nerves): with an experimental study of their functions. J Bone Joint Surg Am 1956;38-A(2):377–91. https://doi.org/10.2106/00004623-195638020-00015.
[10] Lazorthes G, Poulhes J, Espagno J. Etude sur les nerfs sinu-vertébraux lombaires. Le nerf de Roofe existe-t-il? C R Assoc Anat 1947;34:317–20.
[11] Wiberg G. Back pain in relation to the nerve supply of the intervertebral disc. Acta Orthop Scand 1949;19(2):211–21. https://doi.org/10.3109/17453674908991094.
[12] Bogduk N, Tynan W, Wilson AS. The nerve supply to the human lumbar intervertebral discs. J Anat 1981;132(Pt 1):39–56.
[13] Raoul S, Faure A, Robert R, Rogez JM, Hamel O, Cuillère P, et al. Role of the sinu-vertebral nerve in low back pain and anatomical basis of therapeutic implications. Surg Radiol Anat 2003;24(6):366–71. https://doi.org/10.1007/s00276-002-0084-8.
[14] Zhao Q, Cheng L, Yan H, Deng S, Zhao J, Liu Z, et al. The anatomical study and clinical significance of the sinuvertebral nerves at the lumbar levels. Spine (Phila Pa 1976) 2020;45(2):E61–6. https://doi.org/10.1097/BRS.0000000000003190.

[15] Shayota B, Wong TL, Fru D, David G, Iwanaga J, Loukas M, et al. A comprehensive review of the sinuvertebral nerve with clinical applications. Anat Cell Biol 2019;52(2):128–33. https://doi.org/10.5115/acb.2019.52.2.128.

[16] Vos T, Flaxman AD, Naghavi M, Lozano R, Michaud C, Ezzati M, et al. Years lived with disability (YLDs) for 1160 sequelae of 289 diseases and injuries 1990-2010: a systematic analysis for the Global Burden of Disease Study 2010. Lancet 2012;380(9859):2163–96. https://doi.org/10.1016/S0140-6736(12)61729-2.

[17] Dutmer AL, Schiphorst Preuper HR, Soer R, Brouwer S, Bültmann U, Dijkstra PU, et al. Personal and societal impact of low back pain: The Groningen Spine Cohort. Spine (Phila Pa 1976) 2019;44(24):E1443–51. https://doi.org/10.1097/BRS.0000000000003174.

[18] Manchikanti L, Singh V, Pampati V, Damron KS, Barnhill RC, Beyer C, et al. Evaluation of the relative contributions of various structures in chronic low back pain. Pain Physician 2001;4(4):308–16.

[19] Parker SL, Mendenhall SK, Godil SS, Sivasubramanian P, Cahill K, Ziewacz J, et al. Incidence of low back pain after lumbar discectomy for herniated disc and its effects on patient-reported outcomes. Clin Orthop Relat Res 2015;473(6):1988–99. https://doi.org/10.1007/s11999-015-4193-1.

[20] Nakamura S, Takahashi K, Takahashi Y, Morinaga T, Shimada Y, Moriya H. Origin of nerves supplying the posterior portion of lumbar intervertebral discs in rats. Spine (Phila Pa 1976) 1996;21(8):917–24. https://doi.org/10.1097/00007632-199604150-00003.

[21] Ohtori S, Takahashi Y, Takahashi K, Yamagata M, Chiba T, Tanaka K, et al. Sensory innervation of the dorsal portion of the lumbar intervertebral disc in rats. Spine (Phila Pa 1976) 1999;24(22):2295–9. https://doi.org/10.1097/00007632-199911150-00002.

[22] Ohtori S, Takahashi K, Chiba T, Yamagata M, Sameda H, Moriya H. Sensory innervation of the dorsal portion of the lumbar intervertebral discs in rats. Spine (Phila Pa 1976) 2001;26(8):946–50. https://doi.org/10.1097/00007632-200104150-00020.

[23] Jinkins RJ. The anatomic and physiologic basis of local, referred and radiating lumbosacral pain syndromes related to disease of the spine. J Neuroradiol 2004;31:163–80. https://doi.org/10.1016/s0150-9861(04)96988-x.

[24] Edgar MA. The nerve supply of the lumbar intervertebral disc. J Bone Joint Surg Br 2007;89(9):1135–9 Erratum in: J Bone Joint Surg Br 2008;90(4):543. https://doi.org/10.1302/0301-620X.89B9.18939.

[25] Richardson J, Collinghan N, Scally AJ, Gupta S. Bilateral L1 and L2 dorsal root ganglion blocks for discogenic low-back pain. Br J Anaesth 2009;103(3):416–9. https://doi.org/10.1093/bja/aep166.

[26] Van Tilburg CWJ, Stronks DL, Groeneweg JG, Huygen FJPM. Randomized sham-controlled, double-blind, multicenter clinical trial on the effect of percutaneous radiofrequency at the ramus communicans for lumbar disc pain. Eur J Pain 2017;21(3):520–9. https://doi.org/10.1002/ejp.945.

[27] Golub BS, Silverman B. Transforaminal ligaments of the lumbar spine. J Bone Joint Surg Am 1969;51(5):947–56. https://doi.org/10.2106/00004623-196951050-00011.

[28] Fardon DF, Williams AL, Dohring EJ, Murtagh FR, Gabriel Rothman SL, Sze GK. Lumbar disc nomenclature: version 2.0: Recommendations of the combined task forces of the North American Spine Society, the American Society of Spine Radiology and the American Society of Neuroradiology. Spine J 2014;14(11):2525–45. https://doi.org/10.1016/j.spinee.2014.04.022.

[29] Hsu SM, Raine L, Fanger H. A comparative study of the peroxidase-antiperoxidase method and an avidin-biotin complex method for studying polypeptide hormones with radioimmunoassay antibodies. Am J Clin Pathol 1981;75(5):734–8. https://doi.org/10.1093/ajcp/75.5.734.

[30] Bridge CJ. Innervation of spinal meninges and epidural structures. Anat Rec 1959;133(3):553–63. https://doi.org/10.1002/ar.1091330308.

[31] Pope JE, Deer TR, Kramer J. A systematic review: current and future directions of dorsal root ganglion therapeutics to treat chronic pain. Pain Med 2013;14(10):1477–96. https://doi.org/10.1111/pme.12171.

[32] Dass R. Sympathetic components of the dorsal primary divisions of human spinal nerves. Anat Rec 1952;113(4):493–501. https://doi.org/10.1002/ar.1091130410.

[33] Kimmel DL. Innervation of spinal dura mater and dura mater of the posterior cranial fossa. Neurology 1961;11:800–9. https://doi.org/10.1212/wnl.11.9.800.

[34] Oh WS, Shim JC. A randomized controlled trial of radiofrequency denervation of the ramus communicans nerve for chronic discogenic low back pain. Clin J Pain 2004;20(1):55–60. https://doi.org/10.1097/00002508-200401000-00011.

[35] Simopoulos TT, Malik AB, Sial KA, Elkersh M, Bajwa ZH. Radiofrequency lesioning of the L2 ramus communicans in managing discogenic low back pain. Pain Physician 2005;8(1):61–5.

[36] Murata Y, Kato Y, Miyamoto K, Takahashi K. Clinical study of low back pain and radicular pain pathways by using L2 spinal nerve root infiltration: a randomized, controlled, clinical trial. Spine (Phila Pa 1976) 2009;34(19):2008–13. https://doi.org/10.1097/BRS.0b013e3181b1fb96.

[37] Rigaud J, Riant T, Labat J, Guerineau M, Robert R. Is section of the sympathetic rami communicantes by laparoscopy in patients with refractory low back pain efficient? Eur Spine J 2013;22(4):775–81. https://doi.org/10.1007/s00586-012-2507-5.

[38] García-Cosamalón J, del Valle ME, Calavia MG, García-Suárez O, López-Muñiz A, Otero J, et al. Intervertebral disc, sensory nerves and neurotrophins: who is who in discogenic pain? J Anat 2010;217(1):1–15. https://doi.org/10.1111/j.1469-7580.2010.01227.x.

[39] Heilingoetter CL, Jensen MB. Histological methods for ex vivo axon tracing: a systematic review. Neurol Res 2016;38(7):561–9. https://doi.org/10.1080/01616412.2016.1153820.

[40] Amonoo-Kuofi HS, el-Badawi MG, Fatani JA. Ligaments associated with lumbar intervertebral foramina. 1. L1 to L4. J Anat 1988;156:177–83.

[41] Mirkovic S, Schwartz DG, Glazier KD. Anatomic considerations in lumbar posterolateral percutaneous procedures. Spine (Phila Pa 1976) 1995;20(18):1965–71. https://doi.org/10.1097/00007632-199509150-00001.

[42] Harms JG, Jeszenszky J. Die posteriore, lumbale, interkorporelle Fusion in unilateraler transforaminaler Technik. Oper Orthop Traumatol 1998;10(2):90–102. https://doi.org/10.1007/s00064-006-0112-7.

[43] Tumialán LM, Madhavan K, Godzik J, Wang MY. The history of and controversy over Kambin's triangle: a historical analysis of the lumbar transforaminal corridor for endoscopic and surgical approaches. World Neurosurg 2019;123:402–8. https://doi.org/10.1016/j.wneu.2018.10.221.